PAPER

NJC
www.rsc.org/njc

Synthesis and characterization of two metal phosphonates with 3D structures: $Cu^{I}_2Cu^{II}[(3\text{-}C_5H_4N)CH(OH)PO_3]_2$ and $Zn[(3\text{-}C_5H_4N)CH(OH)PO_3]$

Deng-Ke Cao, Yong-Jiang Liu, You Song and Li-Min Zheng*

State Key Laboratory of Coordination Chemistry, Coordination Chemistry Institute, Nanjing University, Nanjing, 210093, P. R. China. E-mail: lmzheng@netra.nju.edu.cn; Fax: +86-25-83314502

Received (in Montpellier, France) 21st October 2004, Accepted 19th January 2005
First published as an Advance Article on the web 30th March 2005

Two novel phosphonate compounds, $Cu^{I}_2Cu^{II}[(3\text{-}C_5H_4N)CH(OH)PO_3]_2$ (**1**) and $Zn[(3\text{-}C_5H_4N)CH(OH)PO_3]$ (**2**), have been synthesized by solvothermal reactions of the corresponding metal salts with [hydroxy (3-pyridyl)methyl]phosphonic acid. Compound **1** contains inorganic chains made up of $Cu^{II}O_4$ planes and CPO_3 tetrahedra through corner sharing. These chains are connected by $Cu^{I}ON$ units through pyridine rings, forming a 3D open framework structure. Compound **2** adopts a new type of pillared layered structure. The inorganic layer contains 8- and 16-membered rings made up of ZnO_3N and CPO_3 tetrahedra. Pyridine rings are fixed between the inorganic layers through covalent bonds. The magnetic study shows that weak ferromagnetic interactions are mediated between magnetic centers in compound **1**.

DOI: 10.1039/b416276e

The past two decades has witnessed a rapid growth in metal phosphonate chemistry due to potential applications in catalysis, ion exchange, sensors, *etc*.[1–6] Attention has been particularly focused on the exploration of new materials with novel polymeric structures. Among the diversity of metal phosphonate compounds, those containing additional functional groups such as carboxylato, sulfonato, amino, crown ether and a second phosphonate unit are of particular interest.[5,7–13] It is anticipated that the introduction of additional functional groups into the phosphonate ligand will not only provide new types of structures, but also confer interesting microporous, catalytic and/or magnetic properties onto the phosphonate materials.[14–20] For compounds containing pyridyl groups, Lin *et al*. reported several metal phosphonate compounds with 1D, 2D and 3D architectures based on 3- and 4-pyridylphosphonate.[21] By using [hydroxy(4-pyridyl)methyl]phosphonate, in which a chiral carbon is inserted between the pyridyl and phosphonate groups, we have recently reported three achiral isostructural compounds of the type $[M(4\text{-}C_5H_4N)CH(OH)PO_3](H_2O)$, with M = Mn, Fe, Co, showing layered structures.[22] Although [hydroxy(3-pyridyl)methyl]phosphonate only differs from [hydroxy(4-pyridyl)methyl]phosphonate by the substitution position of the pyridyl ring, it results in completely different structures when reacted with metal salts. Herein, we describe the hydrothermal synthesis and structural characterization of two novel compounds based on [hydroxy (3-pyridyl)methyl]phosphonate, namely, $Cu^{I}_2Cu^{II}[(3\text{-}C_5H_4N)CH(OH)PO_3]_2$ (**1**) and $Zn[(3\text{-}C_5H_4N)CH(OH)PO_3]$ (**2**). The magnetic properties of compound **1** are also investigated.

Experimental

Materials and instruments

[Hydroxy(3-pyridyl)methyl]phosphonic acid (3-hpmpH_2) was synthesized according to the literature.[23] All starting materials were of reagent grade quality and were obtained from commercial sources without further purification. Elemental analysis was performed on a Perkin Elmer 240C elemental analyzer. The IR spectra were obtained from KBr pellets on a VECTOR 22 spectrometer. Variable temperature magnetic susceptibility data for **1** were obtained from a polycrystalline sample and measured in the temperature range 2–300 K using a Quantum Design SQUID magnetometer. Diamagnetic corrections were estimated from Pascal's constants.[24]

Syntheses

$Cu_3[(3\text{-}C_5H_4N)CH(OH)PO_3]_2$ (1). A mixture of $CuSO_4$ (0.0272 g, 0.17 mmol) and 3-hpmpH_2 (0.0473 g, 0.25 mmol) in 8 ml H_2O and 2 ml C_2H_5OH, adjusted to pH = 5.35 with 1 M NaOH, was kept in a Teflon-lined autoclave at 140 °C for 24 h (final pH = 4.50). After cooling to room temperature, green needle-like crystals of **1** were collected as a monophasic material, based on powder X-ray diffraction analysis. Yield: 0.019 g (59% based on Cu). Anal. calcd for $C_{12}H_{12}N_2O_8P_2Cu_3$: C, 25.50; H, 2.12; N, 4.96; found: C, 24.92; H, 1.84; N, 4.91%. IR (KBr, cm^{-1}): 3445 (s, br), 3080 (w), 1638 (m), 1604 (m), 1480 (w), 1425 (m), 1295 (w), 1211 (w), 1184 (m), 1100 (s), 1074 (s), 1045 (s), 991 (s), 827 (m), 802 (m), 759 (m), 703 (m), 660 (w), 592 (m), 558 (m), 505 (w), 443 (w), 361 (w).

$Zn[(3\text{-}C_5H_4N)CH(OH)PO_3]$ (2). A mixture of $ZnSO_4 \cdot 7H_2O$ (0.0489 g, 0.17 mmol) and 3-hpmpH_2 (0.0473 g, 0.25 mmol) in 8 ml H_2O and 2 ml EtOH, adjusted to pH = 4.63 with 1 M NaOH, was kept in a Teflon-lined autoclave at 140 °C for 24 h (final pH = 3.67). After cooling to room temperature, colorless blocky crystals of **2** were collected as a monophasic material, based on powder X-ray diffraction analysis. Yield: 0.041 g (95% based on Zn). Anal. calcd for $C_6H_6NO_4PZn$: C, 28.52; H, 2.38; N, 5.55; found: C, 28.40; H, 2.23; N, 5.43%. IR (KBr, cm^{-1}): 3363 (m, br), 3262 (m, br), 3055 (w), 1609 (m), 1482 (w), 1436 (m), 1340 (w), 1273 (w), 1233 (w), 1209 (w), 1143 (m), 1126 (m), 1083 (s), 1054 (s), 1002 (s), 860 (w), 834 (w), 764 (w), 709 (m), 667 (w), 657 (w), 567 (m), 524 (w), 465 (w), 418 (w).

X-Ray crystallography

Single crystals of dimensions 0.10 × 0.04 × 0.04 mm^3 for **1** and 0.05 × 0.03 × 0.02 mm^3 for **2** were used for structural determination on a Bruker SMART APEX CCD diffractometer using graphite-monochromated MoKα radiation (λ = 0.710 73 Å) at room temperature. Data were integrated using the Siemens SAINT program,[25] with the intensities corrected for Lorentz factor, polarization, air absorption, and absorption due to variation in the path length through the detector faceplate. Empirical absorption corrections were applied. The structures were solved by direct methods and refined on F^2 by full-matrix least squares using SHELXTL.[26] All the nonhydrogen atoms were located from the Fourier maps and were refined anisotropically. All H atoms were refined isotropically, with the isotropic vibration parameters related to the non-H atom to which they are bonded. For compound **2**, the hydroxy group is disordered over two sites [O(4), O(4′)]. The H atom attached to C(6) was not located.

Results and discussion

X-Ray crystallographic characterization

Selected crystallographic data and refinement parameters for compounds **1** and **2** are given in Table 1.†

Structure of $Cu^{I}_2Cu^{II}[(3\text{-}C_5H_4N)CH(OH)PO_3]_2$ (1). Compound **1** crystallizes in the monoclinic space group $P2_1/c$. The asymmetric unit contains two crystallographically independent Cu atoms. The Cu(1) atom is divalent and is located at the special position (0, 0.5, 0.5), while the Cu(2) atom is monovalent and resides at a general position. The bond valence sums for the Cu(1) and Cu(2) atoms are 1.90 and 1.07, respectively.[27] The geometry around Cu(1) can be described as a slightly distorted square planar. All four coordination sites are filled by four phosphonate oxygens [O(1), O(1A), O(3B) and O(3C)] from four equivalent 3-hpmp^{2-} ligands. Selected bond lengths and angles are given in Table 2. The Cu(1)–O bond lengths fall in the range 1.924(3)–1.987(3) Å. The deprotonated 3-hpmp^{2-} acts as a tetradentate ligand. It bridges the equivalent Cu(1) atoms by using two of its three phosphonate oxygens, O(1) and O(3), forming a paramagnetic linear chain of $\{Cu^{II}[(3\text{-}C_5H_4N)CH(OH)PO_3]_2\}_n$ along the [100] direction (Fig. 1). The Cu(1)···Cu(1A) distance within the chain is 4.788(1) Å. The remaining phosphonate oxygen atom O(2) and the pyridyl nitrogen atom N(1) are both coordinated to the monovalent Cu(2) atom. The coordination geometry around Cu(2) is almost linear, considering that the O(2)–Cu(2)–N(1D) bond angle is 174.7(1)°. The Cu(2)–O(2) and Cu(2)–N(1D) distances are 1.808(3) and 1.859(4) Å, respectively.

Fig. 2 shows the packing diagram of compound **1**. Clearly, the monovalent Cu(2) atom acts as a linker and connects the paramagnetic chains of $\{Cu^{II}[(3\text{-}C_5H_4N)CH(OH)PO_3]_2\}_n$ in four directions. As a consequence, a new type of metal phosphonate open framework structure is built up. The hydroxy group of the 3-hpmp^{2-} ligand is involved in hydrogen bonding with the phosphonate oxygen atom O(3) [O(4)···O(3)^{i}: 2.743(4) Å, symmetry code: i, $-x+1$, $-y+1$, $-z+1$].

Table 1 Crystallographic data and refinement parameters for compounds **1** and **2**

Compound	**1**	**2**
Empirical formula	$C_{12}H_{12}N_2O_8P_2Cu_3$	$C_6H_6NO_4PZn$
FW	564.80	252.46
Crystal system	Monoclinic	Monoclinic
Space group	$P2_1/c$	$P2_1/c$
a/Å	4.7881(7)	8.694(2)
b/Å	11.948(2)	9.210(2)
c/Å	13.991(2)	10.062(2)
β/°	96.431(3)	111.750(4)
U/Å^3	759.4(2)	748.3(3)
Z	2	4
ρ_{calcd}/g cm^{-3}	2.358	2.241
Reflections collected	4772	4584
Unique reflections	1847	1862
R_{int}	0.0348	0.0766
R_1 [$I > 2\sigma(I)$][a]	0.0430	0.0523
wR_2 [$I > 2\sigma(I)$][a]	0.1114	0.0837
R_1 (All data)[a]	0.0556	0.1016
wR_2 (All data)[a]	0.1153	0.0937

[a] $R_1 = \sum||F_o| - |F_c||/\sum|F_o|$; $wR_2 = [\sum w(F_o^2 - F_c^2)^2/\sum w(F_o^2)^2]^{1/2}$

Table 2 Selected bond lengths (Å) and angles (°) for **1**[a]

Cu(1)–O(1)	1.924(3)	O(1)–Cu(1)–O(3B)	88.4(1)
Cu(1)–O(3B)	1.987(3)	O(1)–Cu(1)–O(3C)	91.6(1)
Cu(2)–O(2)	1.808(3)	O(2)–Cu(2)–N(1D)	174.7(2)
Cu(2)–N(1D)	1.859(4)	C(5)–N(1)–Cu(2F)	121.3(3)
P(1)–O(1)	1.516(3)	P(1)–O(1)–Cu(1)	133.5(2)
P(1)–O(2)	1.523(3)	P(1)–O(2)–Cu(2)	128.8(2)
P(1)–O(3)	1.526(3)	P(1)–O(3)–Cu(1E)	122.4(2)
P(1)–C(6)	1.825(4)	C(1)–N(1)–Cu(2F)	121.4(3)

[a] Symmetry transformations used to generate equivalent atoms: A: $-x$, $-y+1$, $-z+1$; B: $x-1$, y, z; C: $-x+1$, $-y+1$, $-z+1$; D: $-x$, $y+1/2$, $-z+1/2$; E: $x+1$, y, z; F: $-x$, $y-1/2$, $-z+1/2$.

Structure of $Zn[(3\text{-}C_5H_4N)CH(OH)PO_3]$ (2). Compound **2** also crystallizes in the monoclinic space group $P2_1/c$. However, it shows a completely different structure from compound **1**. The asymmetric unit of **2** consists of one Zn atom and one 3-hpmp^{2-} ligand (Fig. 3). The Zn atom has a distorted tetrahedral environment. Three of the four coordination sites are occupied by O(1), O(2A) and O(3B) from three equivalent phosphonate ligands. A pyridyl nitrogen, N(1C), from the forth equivalent phosphonate ligand, fills the remaining site. Selected bond lengths and angles are given in Table 3. The Zn(1)–O(N) bond lengths are 1.922(4)–2.029(4) Å while the angles around the Zn atom range from 98.2(2)° to 117.5(2)°. The 3-hpmp^{2-} ligand is again tetradentate. The three phosphonate

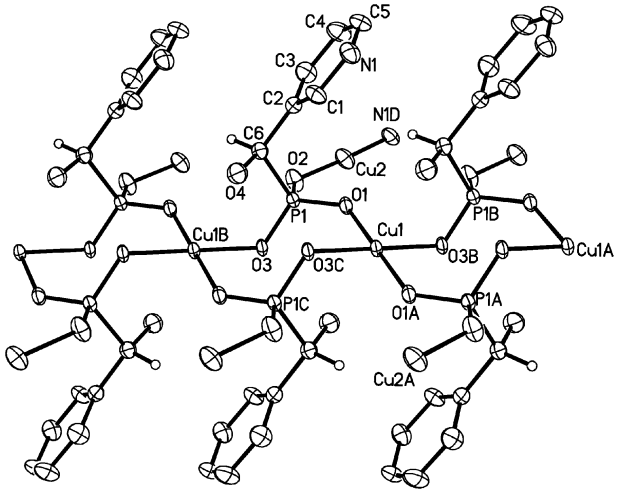

Fig. 1 A fragment of the paramagnetic linear chain in **1** with atom labelling scheme (50% probability). All H atoms except H(6A) are omitted for clarity.

† CCDC reference numbers: 251889 and 251890. See http://www.rsc.org/suppdata/nj/b4/b416276e/ for crystallographic data in .cif or other electronic format.

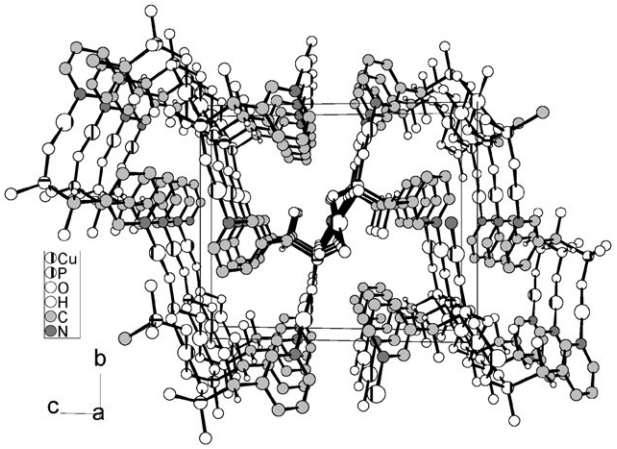

Fig. 2 Packing diagram of **1** viewed along the *a* axis.

oxygens, however, are each coordinated to a single Zn atom and *vice versa*, forming an inorganic layer containing 8- and 16-membered rings (Fig. 4). To our knowledge, such a layer has not been observed in other metal phosphonates with layered or pillared layered structures. The pyridyl nitrogen atom completes the coordination sphere around the Zn atom, while connecting the inorganic layers into a new type of pillared layered structure (Fig. 5).

The structures of compounds **1** and **2** are entirely new compared to other reported copper and zinc monophosphonates such as $M(O_3PR)\cdot H_2O$ (M = Cu, Zn; R = CH_3, C_6H_5, C_2H_5),[28–31] $Cu_3[(O_3PCH_2)_2NH_2]_2$,[32] $Na[Cu(O_3P(CH_2)_2CO_2)]$,[7] $Zn(O_3PC_2H_4NH_2)$,[33] $Zn_3(O_3PC_2H_4CO_2)_2$ and $Zn(O_3PC_2H_4CO_2H)\cdot 1.5H_2O$.[34] They are also different from those involving functional pyridyl groups. To date, there are only several examples of metal phosphonate compounds in which the phosphonate ligands are attached to pyridyl groups. Compound Zn(3-pyridylphosphonate)(Br) shows a double chain structure in which the pyridyl nitrogen is protonated.[21] Compound $[Cu^{II}_2(4\text{-pyridylphosphonate})_2]\cdot 2H_2O$ has a 3D framework structure with rectangular channels.[21] In compounds $[M(4\text{-}C_5H_4N)CH(OH)PO_3](H_2O)$ (M = Mn, Fe, Co, Zn, Cd),[22,35] the inorganic double chains are connected by pyridyl groups into a 2D layer.

The structural differences between compounds **1** and **2** can be caused by the different coordination modes of the metal ions. The Zn(II) ion favors a tetrahedral arrangement while the Cu(II) ion prefers a square or square-pyramidal geometry due to Jahn–Teller effects. The partial reduction of Cu(II) into Cu(I) leads to the formation of a mixed-valent compound. To the best of our knowledge, this is only the third example of a mixed-valent copper(I,II) phosphonate. The other two are $Na_2Cu_{15}(hedp)_6(OH)_2(H_2O)$[36] and $Cu_2^{I}Cu^{II}(hedpH_2)_2(4,4'\text{-bipy})_2\cdot 2H_2O$.[37] Furthermore, compound **1** contains paramagnetic chains of Cu(II), doubly linked by O–P–O bridges, which are well isolated from each other by diamagnetic pyridyl

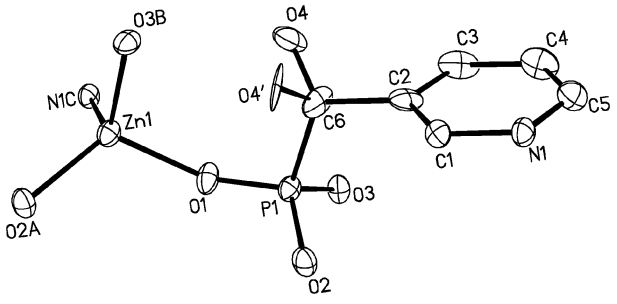

Fig. 3 Structure building unit of **2** with atom labelling scheme (50% probability). All H atoms are omitted for clarity.

Table 3 Selected bond lengths (Å) and angles (°) for **2**[a]

Zn(1)–O(2A)	1.922(4)	O(2A)–Zn(1)–O(1)	117.5(2)
Zn(1)–O(1)	1.942(3)	O(2A)–Zn(1)–O(3B)	114.3(2)
Zn(1)–O(3B)	1.946(4)	O(1)–Zn(1)–O(3B)	106.5(2)
Zn(1)–N(1C)	2.029(4)	O(2A)–Zn(1)–N(1C)	109.2(2)
P(1)–O(1)	1.512(4)	O(1)–Zn(1)–N(1C)	98.2(2)
P(1)–O(2)	1.513(4)	O(3B)–Zn(1)–N(1C)	109.7(2)
P(1)–O(3)	1.528(4)	P(1)–O(1)–Zn(1)	144.4(2)
P(1)–C(6)	1.823(6)	P(1)–O(2)–Zn(1A)	125.7(2)
		P(1)–O(3)–Zn(1D)	140.9(2)
		C(5)–N(1)–Zn(1E)	118.1(4)
		C(1)–N(1)–Zn(1E)	124.4(4)

[a] Symmetry transformations used to generate equivalent atoms: A: $-x+2, -y, -z+1$; B: $x, -y+1/2, z-1/2$; C: $x+1, y, z$; D: $x, -y+1/2, z+1/2$; E: $x-1, y, z$.

groups and Cu(I) ions. It therefore offers an ideal case of O–P–O bridged copper chains that allows for a detailed magnetic investigation.

Magnetic properties of 1

The temperature-dependent molar magnetic susceptibility of **1** was measured at 2 kOe in the temperature range 2–300 K. The room temperature effective magnetic moment of 1.87 μ_B is close to the expected spin-only value for spin $S = 1/2$ (1.73 μ_B). Above 50 K, the magnetic behavior follows the Curie–Weiss law with a Curie constant of 0.43 cm^3 K mol^{-1}. The positive Weiss constant (+7.6 K) and the continuous increase of $\chi_M T$ upon cooling indicate ferromagnetic interactions between adjacent Cu(II) ions. The magnetic susceptibility data were analyzed by a uniform ferromagnetic chain model for $S = 1/2$, based on the Heisenberg Hamiltonian $H = -J\,\Sigma S_{Ai}S_{Ai+1}$:[24]

$$\chi'_M = \frac{Ng^2\beta^2}{4kT}\left(\frac{N}{D}\right)^{\frac{2}{3}}$$

with

$$N = 1.0 + 5.7979916y + 16.902653y^2 + 29.376885y^3 + 29.832959y^4 + 14.036918y^5$$

$$D = 1.0 + 2.7979916y + 7.0086780y^2 + 8.6538644y^3 + 4.5743114y^4$$

where $y = J/(2kT)$, J is the coupling constant, and N, g, β and k have their usual meanings. A good fit resulted in parameters $g = 2.17$ and $J = +2.86$ cm^{-1}. If the interchain interaction (zJ') is included, based on the molecular field approximation:

$$\chi_M = \frac{\chi'_M}{1 - zJ'\chi'_M}$$

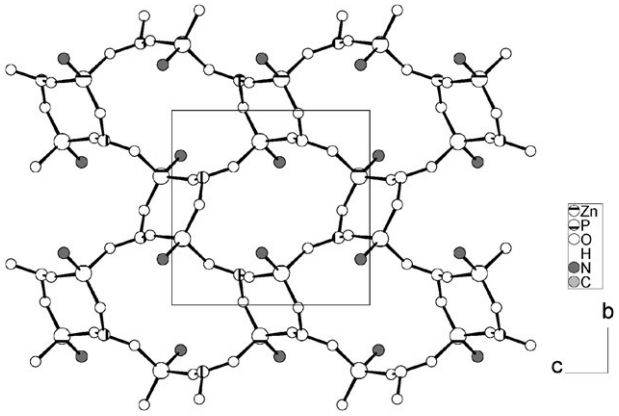

Fig. 4 One inorganic layer of **2** viewed along the *a* axis.

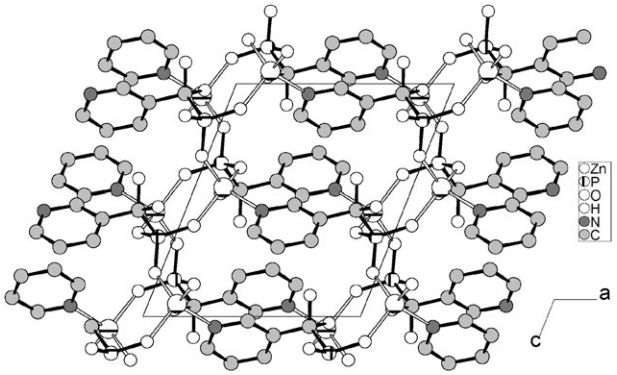

Fig. 5 Packing diagram of **2** viewed along the *b* axis.

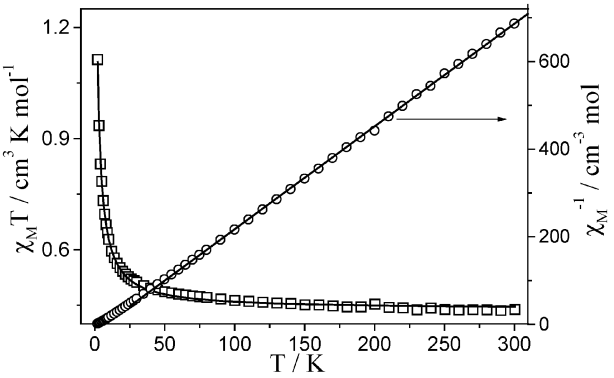

Fig. 6 The $\chi_M T$ (□) and χ_M^{-1} (○) *versus* *T* plots for **1**.

then the parameters become $g = 2.16$ and $J = +3.22$ cm^{-1} and $zJ' = -0.14$ cm^{-1} (Fig. 6). Magnetization curves taken at 2 K showed no evidence of hysteresis, indicating that no long-range magnetic ordering occurred above that temperature. The saturation magnetization at 69.8 kOe (1.11 $N\beta$) is close to the value of 1.08 $N\beta$ anticipated for a spin value of $S = 1/2$ with $g = 2.16$ (Fig. 7).

The observation of dominant ferromagnetic interactions is unusual for metal phosphonate compounds.[38] A few exceptions, however, have been found in a chain compound, $[NH_3CH_2CH_2NH_3]Ni(hedpH_2)_2 \cdot 2H_2O$ [hedp = $CH_3C(OH)(PO_3)_2$],[39] and in a layered compound, $Cu_2(H_2O)_2[O_3PCH_2N(C_2H_4)_2NCH_2PO_3]$,[40] where the metal ions are exclusively linked by O–P–O units. The ferromagnetic exchange couplings in these systems could originate from the accidental orthogonality of the magnetic orbitals. Nevertheless, further investigations are needed in order to fully understand the magnetic behavior of these systems.

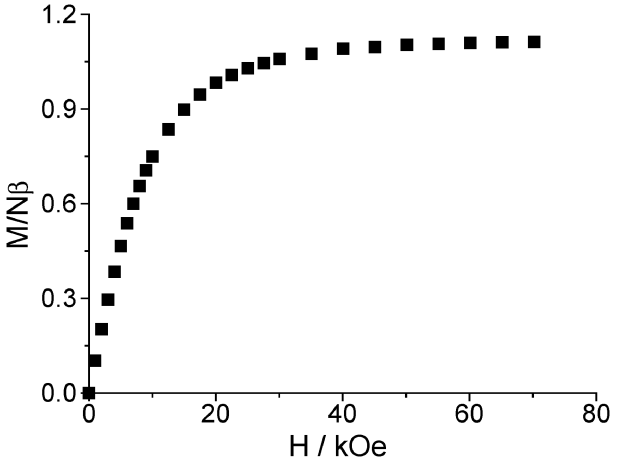

Fig. 7 Field dependent magnetization for compound **1**.

Conclusion

A mixed-valent copper phosphonate, $Cu^{I}_2Cu^{II}\{[(3\text{-}C_5H_4N)CH(OH)PO_3]_2$ (**1**) with an open framework structure, and a zinc phosphonate, $Zn[(3\text{-}C_5H_4N)CH(OH)PO_3]$ (**2**) with a pillared layered structure, are reported in this paper. Weak ferromagnetic interactions are found in compound **1**. The results demonstrate that the introduction of functional groups such as pyridyl can have a significant influence on the structures and, therefore, the properties of the corresponding metal phosphonates. With the aim to finally design and synthesize metal phosphonates with desired structures, more work is required to explore new materials using phosphonate ligands attached with different functional groups.

Acknowledgements

The authors thank the National Natural Science Foundation of China (No. 20325103), the Ministry of Education of China and the Natural Science Foundation of Jiangsu province (No. BK2002078) for financial support.

References

1 B. Zhang and A. Clearfield, *J. Am. Chem. Soc.*, 1997, **119**, 2751.
2 G. Alberti, in *Comprehensive Supramolecular Chemistry*, ed. J. M. Lehn, Pergamon, Elesvier Science, Ltd., Oxford, UK, 1996, vol. **7**, pp. 151–187.
3 J. L. Snover, H. Byrd, E. P. Suponeva, E. Vicenzi and M. E. Thompson, *Chem. Mater.*, 1996, **8**, 1490.
4 G. Cao, H. Hong and T. E. Mallouk, *Acc. Chem. Res.*, 1992, **25**, 420.
5 A. Clearfield, *Prog. Inorg. Chem.*, 1998, **47**, 371, and references therein.
6 C. Maillet, P. Janvier, M. Pipelier, T. Praveen, Y. Andres and B. Bujoli, *Chem. Mater.*, 2001, **13**, 2879.
7 M. Riou-Cavellec, M. Sanselme, N. Guillou and G. Ferey, *Inorg. Chem.*, 2001, **40**, 723.
8 N. Stock, G. D. Stucky and A. K. Cheetham, *Chem. Commun.*, 2000, 2277.
9 F. Fredoueil, M. Evain, D. Massiot, M. Bujoli-Doeuff and B. Bujoli, *J. Mater. Chem.*, 2001, **11**, 1106.
10 M. Riou-Cavellec, M. Sanselme, M. Nogues, J. M. Greneche and G. Ferey, *Solid State Sci.*, 2002, **4**, 619.
11 A. Clearfield, D. M. Poojary, B. Zhang, B. Zhao and A. Derecskei-Kovacs, *Chem. Mater.*, 2000, **12**, 2745.
12 J. G. Mao, Z. Wang and A. Clearfield, *Inorg. Chem.*, 2002, **41**, 3713.
13 (*a*) D. M. Poojary, B. Zhang and A. Clearfield, *J. Am. Chem. Soc.*, 1997, **119**, 12550; (*b*) K. Barthelet, M. Nogues, D. Riou and G. Ferey, *Chem. Mater.*, 2002, **14**, 4910; (*c*) E. Burkholder, V. Golub, C. J. O'Connor and J. Zubieta, *Inorg. Chem.*, 2003, **42**, 6729; (*d*) C.-Y. Cheng, S.-J. Fu, C.-J. Yang, W.-H. Chen, K.-J. Lin, G.-H. Lee and Y. Wang, *Angew. Chem., Int. Ed.*, 2003, **42**, 1937; (*e*) E. Dumas, C. Sassoye, K. D. Smith and S. C. Sevov, *Inorg. Chem.*, 2002, **41**, 4029.
14 G. Ferey, *Chem. Mater.*, 2001, **13**, 3084.
15 G. B. Hix, B. M. Kariuki, S. Kitchin and M. Tremayne, *Inorg. Chem.*, 2001, **40**, 1477.
16 M. Jurado-Gonzalez, D. L. Ou, B. Ormsby, A. C. Sullivan and J. R. H. Wilson, *Chem. Commun.*, 2001, 67.
17 A. Hu, H. L. Hgo and W. Lin, *Angew. Chem., Int. Ed.*, 2003, **42**, 6000.
18 C. Bellitto and F. Federici, *Inorg. Chem.*, 2002, **41**, 709.
19 S. O. H. Gutschke, D. J. Price, A. K. Powell and P. T. Wood, *Angew. Chem., Int. Ed.*, 1999, **38**, 1088.
20 P. Yin, S. Gao, L.-M. Zheng, Z. Wang and X.-Q. Xin, *Chem. Commun.*, 2003, 1076.
21 P. Ayyappan, O. R. Evans, B. M. Foxman, K. A. Wheeler, T. H. Warren and W. B. Lin, *Inorg. Chem.*, 2001, **40**, 5954.
22 X.-Y. Yi, L.-M. Zheng, W. Xu and S.-H. Feng, *J. Chem. Soc., Dalton Trans.*, 2003, 953.
23 B. Boduszek, *Tetrahedron*, 1996, **52**, 12483.

24 O. Kahn, *Molecular Magnetism*, VCH Publishers, Inc., New York, 1993.
25 *SAINT, Program for Data Extraction and Reduction*, Siemens Analytical X-ray Instruments, Madison, WI, 1994–1996.
26 G. M. Sheldrick, *SHELXTL Reference Manual*, version 5.0, Siemens Industrial Automation, Analytical Instruments, Madison, WI, 1995.
27 N. E. Brese and M. O'Keeffe, *Acta Crystallogr., Sect. B*, 1991, **47**, 192.
28 Y. Zhang and A. Clearfield, *Inorg. Chem.*, 1992, **31**, 2821.
29 G. Cao, H. Lee, V. M. Lynch and T. E. Mallouk, *Inorg. Chem.*, 1988, **27**, 2781.
30 K. J. Martin, P. J. Squattrito and A. Clearfield, *Inorg. Chim. Acta*, 1989, **155**, 7.
31 G. Cao and T. E. Mallouk, *Inorg. Chem.*, 1991, **30**, 1434.
32 A. Cabeza, S. Bruque, A. Guagliardi and M. A. G. Aranda, *J. Solid State Chem.*, 2001, **160**, 278.
33 S. Drumel, P. Janvier, D. Deniaud and B. Bujoli, *J. Chem. Soc., Chem. Commun.*, 1995, 1051.
34 S. Drumel, P. Janvier, P. Barboux, M. Bujoli-Doeuff and B. Bujoli, *Inorg. Chem.*, 1995, **34**, 148.
35 D.-K. Cao and L.-M. Zheng, unpublished results.
36 L.-M. Zheng, C.-Y. Duan, X.-R. Ye, L.-Y. Zhang, C. Wang and X.-Q. Xin, *J. Chem. Soc., Dalton Trans.*, 1998, 905.
37 L.-M. Zheng, P. Yin and X.-Q. Xin, *Inorg. Chem.*, 2002, **41**, 4084.
38 C. Bellitto, in *Magnetism: Molecules to Materials II: Molecule-Based Materials*, eds. J. S. Miller and M. Drillon, Wiley-VCH Verlag GmbH & Co. KgaA, Weinheim, 2002, pp. 425–456, and references therein.
39 H.-H. Song, L.-M. Zheng, C.-H. Lin, S.-L. Wang, X.-Q. Xin and S. Gao, *Chem. Mater.*, 1999, **11**, 2382.
40 Y. Wang, S.-S. Bao, W. Xu, J. Chen, S. Gao and L.-M. Zheng, *J. Solid State Chem.*, 2004, **177**, 1297.